

# Conventional Physics Explanations for the NuTeV $\sin^2 \theta_W$

KEVIN S. MCFARLAND\* AND SVEN-OLAF MOCH†

† *Deutsches Elektronensynchrotron DESY  
Platanenallee 6, D-15738 Zeuthen, Germany*

\* *University of Rochester, Rochester, NY 14627 USA*

## Abstract

*The NuTeV experiment has measured  $\sin^2 \theta_W^{(\text{on-shell})} = 0.2277 \pm 0.0013(\text{stat}) \pm 0.0009(\text{syst})$ , approximately 3 standard deviations above the standard model prediction. This discrepancy has motivated speculation that the NuTeV result may be affected significantly by neglected experimental or theoretical effects. We examine the case for a number of proposed explanations.*

## 1 Introduction

The observable  $R^-$

$$R^- \equiv \frac{\sigma(\nu_\mu N \rightarrow \nu_\mu X) - \sigma(\bar{\nu}_\mu N \rightarrow \bar{\nu}_\mu X)}{\sigma(\nu_\mu N \rightarrow \mu^- X) - \sigma(\bar{\nu}_\mu N \rightarrow \mu^+ X)}, \quad (1.1)$$

was first suggested by Paschos and Wolfenstein [1] to measure  $\sin^2 \theta_W$ .

$$R^- \equiv \frac{1}{2} - \sin^2 \theta_W \quad (1.2)$$

under the assumptions of equal momentum carried by the  $u$  and  $d$  valence quarks in the target and of equal momentum carried by the heavy quark and anti-quark seas. The Paschos-Wolfenstein numerator and denominator are independent of the sea quark momenta since  $\sigma^{\nu q} = \sigma^{\bar{\nu} \bar{q}}$  and  $\sigma^{\bar{\nu} q} = \sigma^{\nu \bar{q}}$ .  $R^-$  is more difficult to measure than the ratio of neutral current to charged current cross-sections,  $R^\nu$ , primarily because the neutral current scattering of  $\nu$  and  $\bar{\nu}$  yield identical observed final states which can only be distinguished through *a priori* knowledge of the initial state neutrino. Therefore, the measurement of  $R^-$  requires separated neutrino and anti-neutrino beams.

As a test of the electroweak predictions for neutrino nucleon scattering, NuTeV has performed a single-parameter fit using its  $R^-$  data to  $\sin^2 \theta_W$  with all other parameters assumed to

have their standard values, e.g., standard electroweak radiative corrections with  $\rho_0 = 1$ . This fit determines

$$\begin{aligned}\sin^2 \theta_W^{(\text{on-shell})} &= 0.22773 \pm 0.00135(\text{stat.}) \pm 0.00093(\text{syst.}) \\ &- 0.00022 \times \left( \frac{M_{\text{top}}^2 - (175 \text{ GeV})^2}{(50 \text{ GeV})^2} \right) \\ &+ 0.00032 \times \ln\left( \frac{M_{\text{Higgs}}}{150 \text{ GeV}} \right).\end{aligned}\quad (1.3)$$

The small dependences in  $M_{\text{top}}$  and  $M_{\text{Higgs}}$  result from radiative corrections as determined from code supplied by Bardin [2] and from V6.34 of ZFITTER [3]; however, it should be noted that these effects are small given existing constraints on the top and Higgs masses [4]. A fit to the precision electroweak data, excluding neutrino measurements, predicts a value of  $0.2227 \pm 0.00037$  [4], approximately  $3\sigma$  from the NuTeV measurement.

The experimental details and theoretical treatment of cross-sections in the NuTeV electroweak measurement are described in detail elsewhere [5]. In brief, NuTeV measures the experimental ratio of neutral current to charged current candidates in both a neutrino and anti-neutrino beam. A Monte Carlo simulation is used to express these experimental ratios in terms of fundamental electroweak parameters. This procedure implicitly corrects for details of the neutrino cross-sections and experimental backgrounds. For the measurement of  $\sin^2 \theta_W$ , the sensitivity arises in the  $\nu$  beam, and the measurement in the  $\bar{\nu}$  beam is the control sample for systematic uncertainties, as suggested in the Paschos-Wolfenstein  $R^-$  of Eqn. (1.1). For simultaneous fits to two electroweak parameters, e.g.,  $\sin^2 \theta_W$  and  $\rho$  or left and right handed couplings, this control of systematics by the Paschos-Wolfenstein  $R^-$  cannot be realized.

### 1.1 Differences between NuTeV and $R^-$

NuTeV does not measure exactly  $R^-$  but rather combinations of experimentally observed neutral-current to charged-current cross-section ratios,  $R^{\text{meas}}$  in neutrino and anti-neutrino beams. Note that  $R^-$  itself can actually be written as

$$R^- \equiv \frac{\sigma(\nu_\mu N \rightarrow \nu_\mu X) - \sigma(\bar{\nu}_\mu N \rightarrow \bar{\nu}_\mu X)}{\sigma(\nu_\mu N \rightarrow \mu^- X) - \sigma(\bar{\nu}_\mu N \rightarrow \mu^+ X)}, \quad (1.4)$$

$$= \frac{\frac{\sigma(\nu_\mu N \rightarrow \nu_\mu X)}{\sigma(\nu_\mu N \rightarrow \mu^- X)} - \frac{\sigma(\bar{\nu}_\mu N \rightarrow \bar{\nu}_\mu X)}{\sigma(\bar{\nu}_\mu N \rightarrow \mu^+ X)} \frac{\sigma(\bar{\nu}_\mu N \rightarrow \mu^+ X)}{\sigma(\nu_\mu N \rightarrow \mu^- X)}}{1 - \frac{\sigma(\bar{\nu}_\mu N \rightarrow \mu^+ X)}{\sigma(\nu_\mu N \rightarrow \mu^- X)}}, \quad (1.5)$$

$$\equiv \frac{R^\nu - r R^{\bar{\nu}}}{1 - r}, \quad (1.6)$$

where  $R$  is the ratio of neutral-current to charged-current total cross-sections and  $r$  is the ratio of charged-current anti-neutrino to neutrino total cross-sections. Therefore,  $R^-$  itself is a combination of  $R$  from neutrino and anti-neutrino beams.

NuTeV does not measure the total cross-section ratios of neutral and charged current interactions. The ratios actually measured by NuTeV,

$$R_{\text{exp}}^\nu = 0.3916 \pm 0.0007 \text{ and } R_{\text{exp}}^{\bar{\nu}} = 0.4050 \pm 0.0016, \quad (1.7)$$

include non-muon neutrino backgrounds, the effects of experimental cuts, cross-talk between candidates in the numerator and denominator and final state effects.

The electron neutrino background can be reliably subtracted as discussed below in Section 2, and the effects of experimental cuts and cross-talk, although large, can be controlled experimentally and introduce no large corrections to the  $R^-$  dependence on  $\sin^2 \theta_W$  as will be shown in Section 4.2.

There are two final state effects which make modest corrections to the NuTeV observables. The first are small differences in acceptance in neutral and charged-current events due to the effect of the final state muon. The second is the effect of the final state in semi-leptonic charm decay. In such decays, some of the final state charmed hadron's energy is carried away in final state neutrinos and some may appear as final state muons. Further complicating the decay, those muons may affect whether the event is measured as a charged-current candidate or neutral-current candidate. These effects are small in the final analysis, but they do make some correction to the NuTeV observables not present in  $R^-$ . Both of these effects are fully modeled and corrected for in the NuTeV analysis.

A more significant difference between NuTeV's analysis and  $R^-$  is the way that  $\sin^2 \theta_W$  is extracted from the two  $R_{\text{exp}}$ . The analysis uses a fit to two parameters,  $\sin^2 \theta_W$  and the effective charm mass,  $m_c$ , in charged-current charm production, which is the largest theoretical uncertainty in the analysis. This  $m_c$  is externally constrained from the NuTeV measurements of charged-current charm production in the two muon final state, and so a 1C fit determines the result of Eqn. (1.3). NuTeV has also performed a fit without this external charm mass constraint [24], and has found

$$\sin^2 \theta_W^{\text{(on-shell)}} = 0.22738 \pm 0.00164(\text{stat.}) \pm 0.00076(\text{syst.}), \quad (1.8)$$

which is consistent with the 1C fit result.

It is instructive to decompose these (linear) fits into combinations of  $R_{\text{exp}}^\nu$  and  $R_{\text{exp}}^{\bar{\nu}}$  in the spirit of Eqn. (1.6). Writing

$$\tilde{R}^- \equiv \frac{R_{\text{exp}}^\nu - a R_{\text{exp}}^{\bar{\nu}}}{b}, \quad \ni' \frac{d\tilde{R}^-}{d\sin^2 \theta_W} = -1 \quad (1.9)$$

where the latter equality holds by choice of  $b$ , we find that for the 1C fit  $a = 0.2492$ ,  $b = 0.6170$ , and for the 0C fit  $a = 0.4526$ ,  $b = 0.6116$ . The similarity between the  $b$  values for the two fits is a statement that the sensitivity to  $\sin^2 \theta_W$  almost entirely resides in  $R_{\text{exp}}^\nu$  and not  $R_{\text{exp}}^{\bar{\nu}}$ , and the near equivalence of the 1C and 0C results indicates that  $R_{\text{exp}}^{\bar{\nu}}$  is in agreement with expectations as is illustrated in Figure 1. The discrepancy with the Standard Model of these results comes then from the fact that  $R_{\text{exp}}^\nu$  is not as expected. Note that these separate measurements, either cast as  $R_{\text{exp}}^\nu$  and  $R_{\text{exp}}^{\bar{\nu}}$  or as the 1C and 0C fits, will constrain any attempt to explain the NuTeV  $\sin^2 \theta_W$  that seeks to make large changes in  $R^\nu$  and  $R^{\bar{\nu}}$  separately to effect a large change in  $R^-$ .

## 2 Experimental Issues

One of the largest experimental corrections to the NuTeV analysis is the subtraction of electron neutrino charged-current events from the neutral current candidate sample. Approximately 5% of the neutral current candidates are electron neutrino charged currents [5], and so a

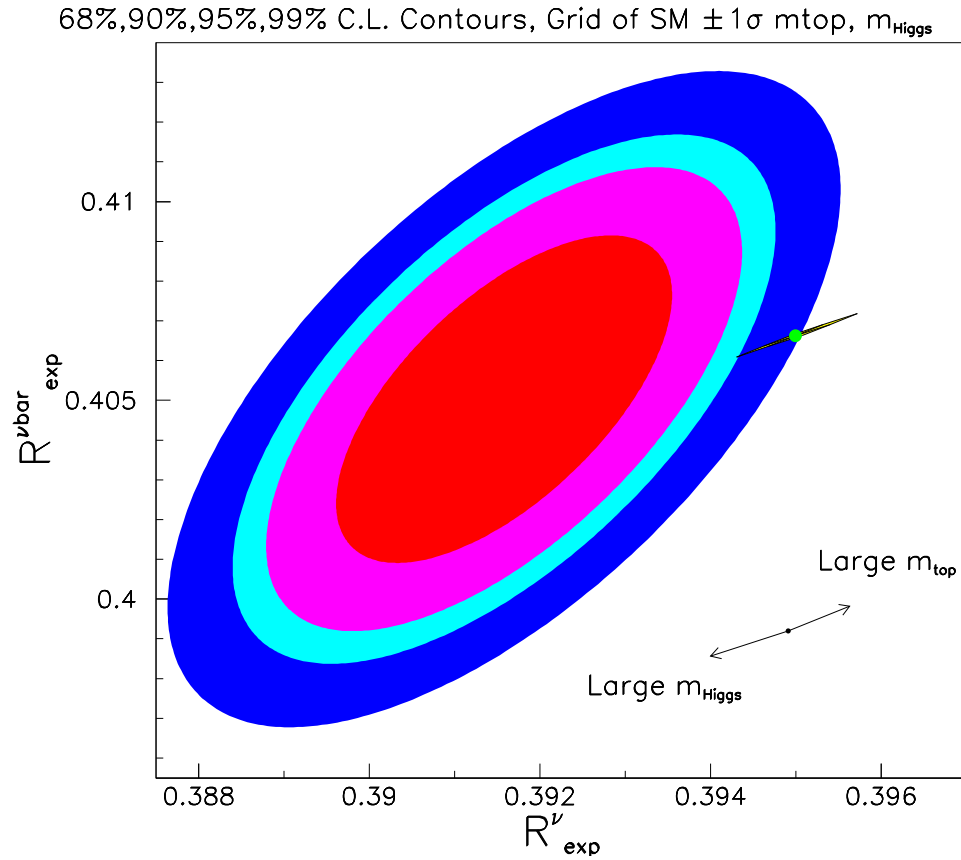


Figure 1: The measurements of  $R_{\text{exp}}^{\nu}$  and  $R_{\text{exp}}^{\nu\text{bar}}$ , shown as an error ellipse. The uncertainties in the error ellipse include theoretical uncertainties in relating  $R_{\text{exp}}^{\nu}$  and  $R_{\text{exp}}^{\nu\text{bar}}$  to fundamental electroweak parameters, which result in the correlation between the two measurements. Note that the  $R_{\text{exp}}^{\nu\text{bar}}$  is in agreement with the Standard Model expectation, shown as the point, whereas the  $R_{\text{exp}}^{\nu}$  measurement is not.

20% overestimate of this rate would be sufficient to explain the difference between the NuTeV  $\sin^2 \theta_W$  and the Standard Model expectation.

The dominant source of electron neutrinos in the NuTeV beams are  $K_{e3}^\pm$  decays. NuTeV determines the electron neutrino background by two methods: one an indirect determination using a beam Monte Carlo tuned to the neutrinos observed from  $K_{\mu 2}^\pm$  decays, and the other a direct, but less precise, measurement of the electron neutrinos [8]. An important check is that the direct and Monte Carlo methods agree, and in fact the ratio of measured to Monte Carlo predicted events is  $1.05 \pm 0.03$  in the neutrino beam and  $1.01 \pm 0.04$  in the anti-neutrino beam.

The largest uncertainty in the Monte Carlo method is the 1.4% fractional uncertainty in the  $K_{e3}^\pm$  branching ratio [9]. An interesting recent development comes from the BNL-E865 experiment which has recently measured a branching ratio for  $K_{e3}^\pm$  [10] that is 6% larger than the value used by NuTeV. If this result is correct, it is interesting to note that it would not disrupt the agreement between the direct and Monte Carlo measurements of the  $\nu_e$  rate at NuTeV and that it would in fact *increase* the discrepancy of the NuTeV  $\sin^2 \theta_W$  with the prediction by slightly less than one standard deviation [24].

The NuTeV observables,  $R_{\text{exp}}^\nu$  and  $R_{\text{exp}}^{\bar{\nu}}$ , have been studied as a function of position within the detector (Figures 2 and 3), the containment length used to separate neutral and charged current candidates (Figure 4) and the visible energy in the detector (Figure 5). Within the statistical and systematic uncertainties of these comparisons, no unexpected deviations as a function of event variables are observed.

### 3 Electroweak Radiative Corrections

NuTeV's analysis includes complete one-loop electroweak radiative corrections [2,3]. These corrections can be separated into those that can be absorbed into effective weak neutral current  $\nu$ - $q$  couplings and those that cannot. The former cause a  $-0.00159$  shift in the NuTeV reported  $\sin^2 \theta_W$ . The latter corrections, dominated by a  $W$ - $\gamma$  box diagram and by acceptance effects from bremsstrahlung in the final-state muon in the charged current shift  $\sin^2 \theta_W$  by an enormous  $-0.00795$ .

One concern about the NuTeV result is that it relies on this single calculation of the radiative corrections. This calculation has been successfully checked against other partial calculations [6, 7] in the limits where both are expected to agree; however, another complete calculation as a cross-check might be advisable.

### 4 QCD corrections

A sizable part of the quoted theoretical error of  $\sin^2 \theta_W$  as determined by NuTeV is due to QCD effects. Therefore, it is mandatory to investigate all potential sources of QCD uncertainties to the best possible accuracy. Sources of QCD effects include parton distributions and their uncertainties, perturbative QCD corrections at higher orders, isospin breaking effects or nuclear effects. In the following, we will discuss these in turn.

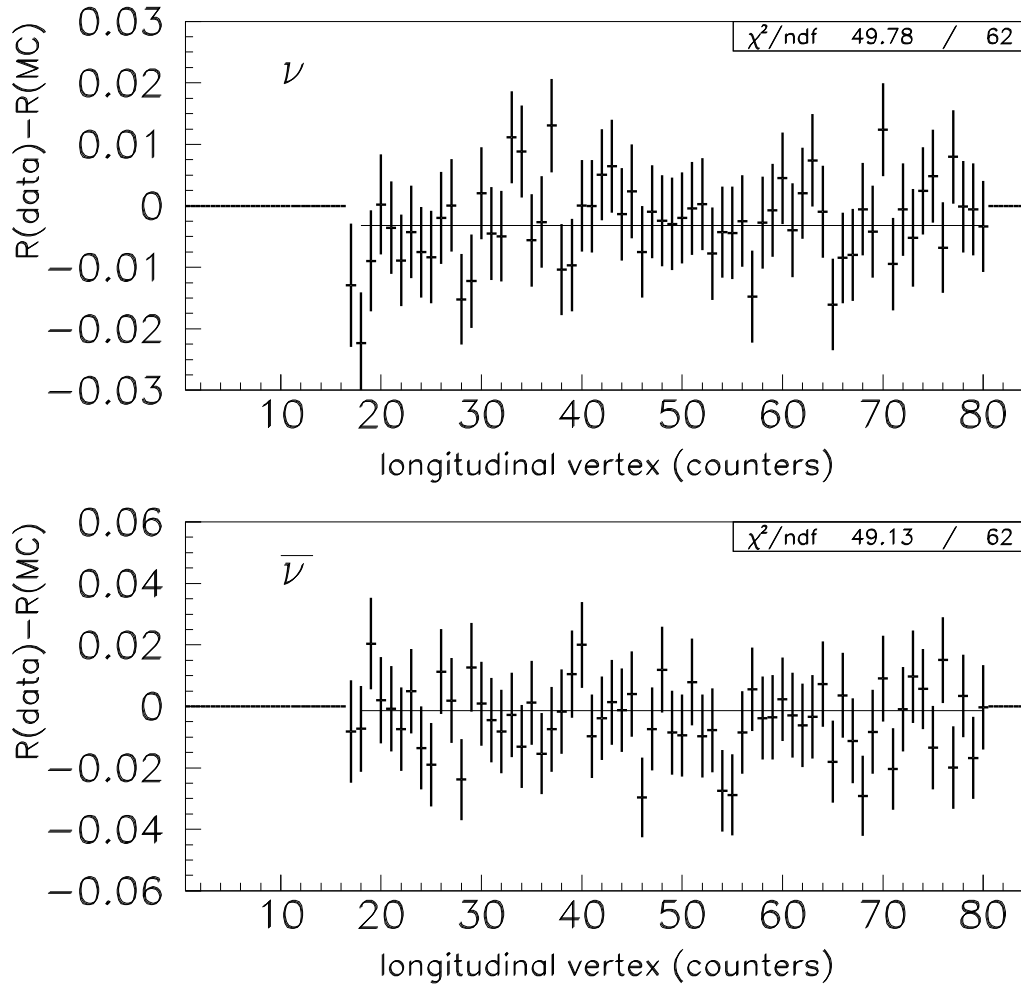


Figure 2: The  $R_{\text{exp}}$  in the neutrino and anti-neutrino beams as a function of the depth of the neutrino interaction within the detector along the beam direction.

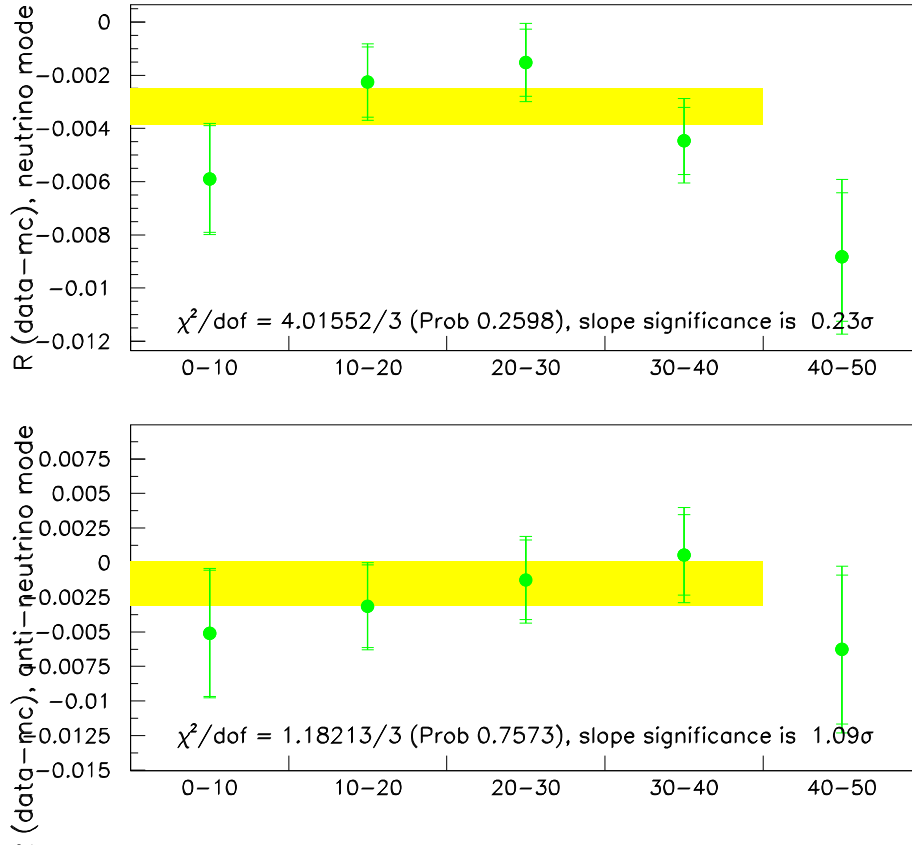


Figure 3: The NuTeV  $R_{\text{exp}}$  binned in square annuli of transverse position from the center to the outer part of the detector. The first four bins are used in this analysis.

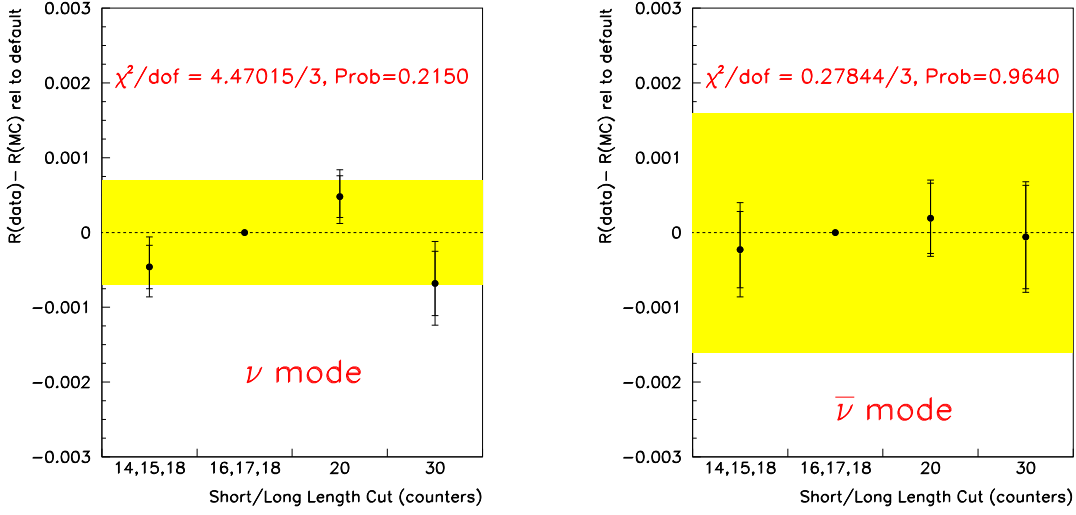


Figure 4: The effect of varying the NuTeV neutral-current/charged-current separation cut on  $R_{\text{exp}}$  in the neutrino (left) and anti-neutrino (right) beams. The error bars represent the statistical uncertainty on the charge. The yellow band is the statistical uncertainty of the ratio as measured from the whole sample.

#### 4.1 Perturbative QCD corrections

The QCD corrections to deep-inelastic scattering at higher orders are long known. For instance, in a complete next-to-leading order (NLO) treatment, and assuming massless quarks, the Paschos–Wolfenstein ratio Eqn. (1.1) becomes<sup>1</sup>

$$R^- = g_L^2 - g_R^2 + \frac{u^- - d^- + c^- - s^-}{u^- + d^-} \left( 3(g_{Lu}^2 - g_{Ru}^2) + (g_{Ld}^2 - g_{Rd}^2) + \frac{8}{9} \frac{\alpha_s}{\pi} (g_L^2 - g_R^2) \right) + \mathcal{O} \left( \frac{1}{(u^- + d^-)^2} \right) + \mathcal{O}(\alpha_s^2). \quad (4.1)$$

Eqn. (4.1) uses the one-loop coefficient functions [13, 14] and holds, if no assumption on the parton content of the target is made. Here  $q^- \equiv q - \bar{q}$  is the second Mellin moment of the corresponding quark and anti-quark distribution,

$$q^- \equiv \int_0^1 dx x (q(x) - \bar{q}(x)). \quad (4.2)$$

For consistency, NLO parton distributions are required, of course, and the nucleon is assumed to contain four light flavors. We will later comment on the treatment of charm as a massive quark.

The result in Eqn. (4.1) has been expanded in powers of the dominant isoscalar combination of parton distributions,  $u^- + d^-$ . It shows the well-known fact, that the Paschos–Wolfenstein relation receives corrections, if the target has an isotriplet component,  $u \neq d$ , or sea quark contributions have a  $C$ -odd component,  $s^- \neq 0$  or  $c^- \neq 0$ . In particular, the QCD corrections only

<sup>1</sup>In ref. [11] the correct value [12] for  $\delta C^1 - 4\delta C^3$  is  $32/9$ , with  $\delta C^1 = C^1 - C^2$  and  $\delta C^3 = C^2 - C^3$ , cf. Eqn. (4.3).

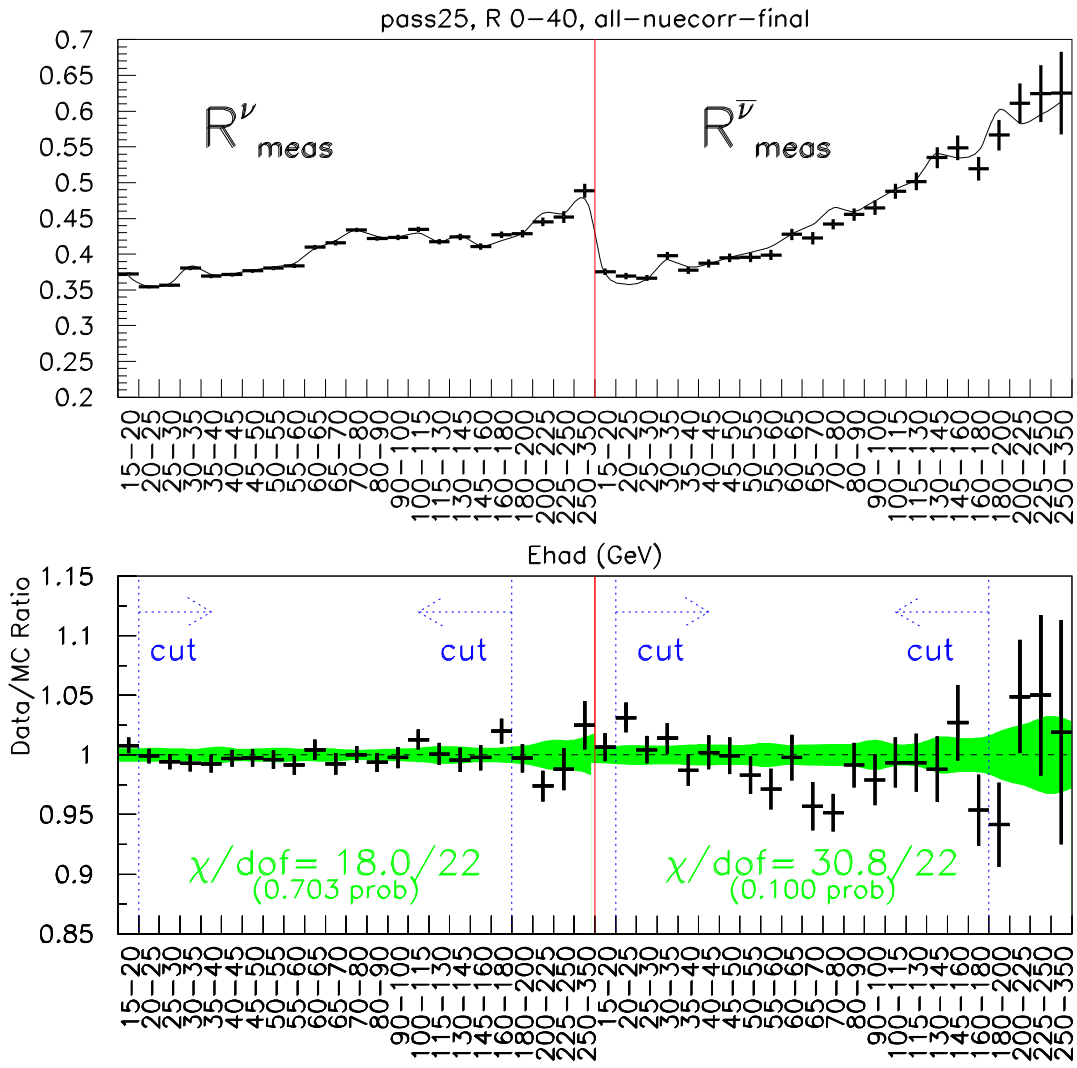


Figure 5: The  $R_{\text{exp}}$  as a function of visible energy in the neutrino and anti-neutrino beams. The ratio of data to Monte Carlo is shown below, with a green band to represent the systematic uncertainties in the comparison.

affect these isotriplet  $u^- - d^-$  and  $C$ -odd terms,  $s^-, c^-$ . It is worth noting, that the coefficient at order  $\alpha_s$  in Eqn. (4.1) is the same in the  $\overline{MS}$ -scheme and the DIS-scheme. This is due to the relevant combination of coefficient functions,

$$-\frac{1}{4}C_{L,q} + C_{2,q} - C_{3,q} \quad (4.3)$$

being invariant under changes between these two schemes. Of course, the NLO parton distributions entering in Eqn. (4.1) differ slightly in the two schemes, most notably in the region of larger  $x$ . Also, it is worth pointing out, that in the combination of coefficient functions in Eqn. (4.3) all dependence on the factorization scale  $\mu_f$  (i.e. all logarithms  $\ln(Q^2/\mu_f^2)$ ) cancels.

Numerically, the correction factor  $\frac{u^- - d^- + c^- - s^-}{u^- + d^-}$  is  $-0.0232$ , evaluated using the NuTeV LO PDFs [5] at the experimental  $Q^2$  which is extracted from fits to CCFR cross-sections [15]. Inclusion of the higher order terms in  $\frac{1}{u^- + d^-}$  changes this to  $-0.0213$ . This evaluation assumes the strange and anti-strange seas carry equal momentum and that PDFs are isospin symmetric (see discussions in Sections 4.3 and 4.5). Therefore, the NLO QCD correction to  $R^-$  is  $-0.00035$ .

It is possible, to extend Eqn. (4.1) to next-to-next-to-leading order (NNLO) in QCD, with the known two-loop coefficient functions [16, 17, 18, 19]. Putting the renormalization and the factorization scales  $\mu_f = \mu_r = Q$ , we find

$$\begin{aligned} R^- &= g_L^2 - g_R^2 + \frac{u^- - d^- + c^- - s^-}{u^- + d^-} \left( 3(g_{Lu}^2 - g_{Ru}^2) + (g_{Ld}^2 - g_{Rd}^2) \right. \\ &\quad \left. + \left\{ \frac{8\alpha_s}{9\pi} + \left[ \frac{5551}{810} - \frac{1}{27}\zeta_2 - \frac{16}{45}\zeta_3 - \frac{83}{162}n_f \right] \frac{\alpha_s^2}{\pi^2} \right\} (g_L^2 - g_R^2) \right) \\ &\quad + \mathcal{O}\left(\frac{1}{(u^- + d^-)^2}\right) + \mathcal{O}(\alpha_s^3), \end{aligned} \quad (4.4)$$

which holds in the  $\overline{MS}$ -scheme. Here,  $n_f$  denotes the number of light (massless) quark flavors, and  $\zeta_2 = 1.644934068$ ,  $\zeta_3 = 1.202056903$ . For arbitrary scales  $\mu_f \neq Q$ , there will be at most single logarithmic dependence on  $Q^2/\mu_f^2$  at order  $\alpha_s^2$  in Eqn. (4.4). All double logarithms  $\ln^2(Q^2/\mu_f^2)$  cancel due to Eqn. (4.3). In the DIS-scheme, the coefficient at order  $\alpha_s^2$  changes slightly. There, the expression in square brackets in Eqn. (4.4) becomes

$$\left[ \frac{8704}{1215} - \frac{5}{9}\zeta_2 - \frac{16}{45}\zeta_3 - \frac{83}{162}n_f \right]. \quad (4.5)$$

Numerically, for typical values of  $\alpha_s$ , the NNLO corrections in both schemes,  $\overline{MS}$  and DIS, are of the order of 30-40 % of the NLO contributions. This shows good perturbative stability of the QCD prediction with respect to higher orders. We have to note however, that a consistent NNLO analysis requires NNLO evolution of the corresponding parton distributions. The necessary three-loop anomalous dimensions are not completely known yet [20, 21].

Thus, we can conclude the pQCD corrections to  $R^-$  are small and that uncertainties due to the perturbative expansion can be reasonably estimated.

## 4.2 Experimental cuts

Because of NuTeV's inability to measure NC events down to zero inelasticity, NuTeV cannot report ratios of total cross sections. One concern, then, is that  $R^-$  may not accurately reflect

NLO QCD corrections to the NuTeV result. In particular, these cuts either remove or change the contributions near the kinematic endpoints in the inelasticity,  $y$ , which is a reason in general where one might expect enhanced sensitivity to radiative corrections.

Backgrounds from sources other than muon neutrino interactions can be reliably subtracted in the NuTeV analysis; however, three major corrections to  $R^-$  remain. These are: (1) the minimum  $\nu$  cut required in order to observe the hadronic recoil in the detector, common to both the charged and neutral current, (2) the difference in the observed visible energy in the charged and neutral current due to the presence of the final state muon, and (3) charged-current events at very low  $E_\mu$  which fake neutral currents. To a significant extent, all of these effects can be modeled by considering the relation (1.1) with cuts on the inelasticity  $y$ .

To that end, let us define for any difference of cross-section the cuts in  $y$  as

$$\left\{ \sigma(\nu_\mu N \rightarrow X) - \sigma(\bar{\nu}_\mu N \rightarrow X) \right\} \Big|_{y_{\min}}^{y_{\max}} = \int_{y_{\min}}^{y_{\max}} dy \frac{d\sigma(\nu_\mu N \rightarrow X)}{dy} - \frac{d\sigma(\bar{\nu}_\mu N \rightarrow X)}{dy} \quad (4.6)$$

with (standard) definition of the inelasticity  $y$  being the fraction of the neutrino's energy lost in the nucleon's rest frame.

A simulation of the effect of the NuTeV broadband flux translates the experimental minimum cut in visible calorimeter energy of 20 GeV into an effective minimum  $y$ -cut,  $y_{\min}$ , of 0.24. Simulations of the energy deposited by the final state muon show a reduction of this effective minimum  $y$  for charged-current events by  $\delta_y$  of 0.03. Finally, a detailed detector and flux simulation [5] can be used to measure the effective  $y$  at which the final state muons in charged-current events are so soft that the events are mistaken for neutral-currents. Denoting this  $y$  at which cross-talk occurs as  $1 - y_X$ ,  $y_X$  is numerically 0.043.

This motivates the definition of a simple cross-section model for  $R^-$  as

$$R_{\text{model}}^-(y_{\min}, \delta y, y_X) \equiv \frac{\left\{ \sigma(\nu_\mu N \rightarrow \nu_\mu X) - \sigma(\bar{\nu}_\mu N \rightarrow \bar{\nu}_\mu X) \right\} \Big|_{y_{\min}}^1 + \left\{ \sigma(\nu_\mu N \rightarrow \mu^- X) - \sigma(\bar{\nu}_\mu N \rightarrow \mu^+ X) \right\} \Big|_{1-y_X}^1}{\left\{ \sigma(\nu_\mu N \rightarrow \mu^- X) - \sigma(\bar{\nu}_\mu N \rightarrow \mu^+ X) \right\} \Big|_{y_{\min}-\delta y}^{1-y_X}} \quad (4.7)$$

which accounts for the kinematic cuts discussed.

We can now work out the structure of  $R_{\text{model}}^-$  including higher order QCD corrections. The result for  $R_{\text{model}}^-$  up to NLO can be written as follows (an extension to NNLO is straight forward):

$$\begin{aligned} R_{\text{model}}^-(y_{\min}, \delta y, y_X) &= f_0(y_{\min}, \delta y, y_X)(g_L^2 - g_R^2) + f_1(y_{\min}, \delta y, y_X) + \frac{u^- - d^- + c^- - s^-}{u^- + d^-} \\ &\times \left( f_u(y_{\min}, \delta y, y_X)(g_{Lu}^2 - g_{Ru}^2) \right. \\ &+ f_d(y_{\min}, y_X)(g_{Ld}^2 - g_{Rd}^2) + f_2(y_{\min}, \delta y, y_X) \\ &\left. + \frac{\alpha_s}{\pi} f_{\alpha_s}(y_{\min}, \delta y, y_X)(g_L^2 - g_R^2) + \frac{\alpha_s}{\pi} f_3(y_{\min}, \delta y, y_X) \right) \end{aligned}$$

$$+\mathcal{O}\left(\frac{1}{(u^- + d^-)^2}\right) + \mathcal{O}(\alpha_s^2), \quad (4.8)$$

where the functions  $f_0, \dots, f_3, f_u, f_d$  and  $f_{\alpha_s}$  are given as

$$\begin{aligned} f_0(y_{\min}, \delta y, y_X) &= \frac{(y_{\min} - 1)(y_{\min}^2 - 2y_{\min} - 2)}{P_1 P_2}, \\ f_1(y_{\min}, \delta y, y_X) &= -\frac{y_X(y_X^2 - 3)}{P_1 P_2}, \\ f_u(y_{\min}, \delta y, y_X) &= -6\frac{(y_{\min} - 1)(y_{\min}^2 - 2y_{\min} - 2)}{P_1 P_2^2}, \\ f_d(y_{\min}, \delta y, y_X) &= -2\frac{(y_{\min} - 1)(y_{\min}^2 - 2y_{\min} - 2)}{P_1 P_2^2} \\ &\quad \times (y_{\min}^2 + y_X^2 + y_X + y_X \delta y + (1 + \delta y)^2 - y_{\min}(2 + y_X + 2\delta y)), \\ f_2(y_{\min}, \delta y, y_X) &= -6\frac{(y_{\min} - 1 - \delta y)y_X(-y_X + y_{\min} - 1 - \delta y)}{P_1 P_2^2}, \\ f_{\alpha_s}(y_{\min}, \delta y, y_X) &= \frac{-\frac{1}{9}(y_{\min} - 1)(y_{\min}^2 - 2y_{\min} - 2)}{P_1 P_2^2} \\ &\quad \times \left( y_{\min}^2 - y_{\min}y_X - 2y_{\min}\delta y - 14y_{\min} \right. \\ &\quad \left. + (13 + \delta y)y_X + 16 + y_X^2 + 14\delta y + \delta y^2 \right), \\ f_3(y_{\min}, \delta y, y_X) &= -\frac{2}{3}\frac{(y_{\min} - 1 - \delta y)y_X}{P_1 P_2^2} \\ &\quad \times (-3y_X + 2y_{\min}y_X - 7 + y_{\min} - \delta y - 2y_X\delta y), \end{aligned} \quad (4.9)$$

where

$$\begin{aligned} P_1 &= y_{\min} - \delta y - 1 + y_X \\ P_2 &= y_X - 2 - y_{\min}y_X + y_X^2 - 2y_{\min} + y_{\min}^2 + 2\delta y + y_X\delta y + \delta y^2 - 2y_{\min}\delta y. \end{aligned} \quad (4.10)$$

In the limit  $y_{\min}, \delta y, y_X \rightarrow 0$  the functions  $f_0, \dots, f_3, f_u, f_d$  and  $f_{\alpha_s}$  simplify to

$$\begin{aligned} f_0(y_{\min}, \delta y, y_X) &= 1, & f_1(y_{\min}, \delta y, y_X) &= 0, \\ f_2(y_{\min}, \delta y, y_X) &= 0, & f_3(y_{\min}, \delta y, y_X) &= 0, \\ f_u(y_{\min}, \delta y, y_X) &= 3, & f_d(y_{\min}, \delta y, y_X) &= 1, \\ f_{\alpha_s}(y_{\min}, \delta y, y_X) &= \frac{8}{9}, \end{aligned} \quad (4.11)$$

in agreement with Eqn. (4.1). Putting in the numerical values from the experimental  $y$  cuts, we find

$$\begin{aligned} f_0(y_{\min}, \delta y, y_X) &= 1.053, & f_1(y_{\min}, \delta y, y_X) &= 0.074, \\ f_2(y_{\min}, \delta y, y_X) &= 0.042, & f_3(y_{\min}, \delta y, y_X) &= 0.038, \\ f_u(y_{\min}, \delta y, y_X) &= 2.700, & f_d(y_{\min}, \delta y, y_X) &= 0.594, \\ f_{\alpha_s}(y_{\min}, \delta y, y_X) &= 0.683, \end{aligned} \quad (4.12)$$

Numerically, then, the NLO QCD correction to  $R_{\text{model}}^-$  is  $-0.00033$ . For comparison, the value for  $dR_{\text{model}}^-/d\sin^2\theta_W$  is  $-1.0075$ . In summary, in this model the experimental cuts in  $y$  do not result in large increases in the  $\mathcal{O}(\alpha_s)$  QCD corrections.

### 4.3 Parton Distribution Functions

Let us next discuss the parton distributions. The very fact, that corrections to  $R^-$  in the QCD improved parton model are proportional to isotriplet or  $C$ -odd components of the nucleon target has led to questions about our knowledge of parton distributions for the various quark flavors. There are two major issues: the isotriplet component introduced by the small neutron excess of the NuTeV target, and possible momentum asymmetries between the strange and anti-strange seas.

The NuTeV analysis corrects for the significant asymmetry of  $d$  and  $u$  quarks that arises because the NuTeV target, which is primarily composed of iron, has a  $\delta N \equiv (A - 2Z)/A = +0.0574 \pm 0.0002$  fractional excess of neutrons over protons. As can be observed from the above uncertainty, the neutron excess is very well known due to a detailed material survey of the NuTeV target, including a chemical assay of the NuTeV steel [22, 23, 24]. The largest uncertainty in this isotriplet correction, in fact, comes from the difference between  $u$  and  $d$  PDFs. From the uncertainty on the NMC  $F_2^d/F_2^p$  [25], NuTeV estimates this uncertainty to be 0.0003 in their extraction of  $\sin^2\theta_W$ . (Note that this correction assumes isospin symmetry, i.e.,  $\binom{-}{u}_p(x) = \binom{-}{d}_n(x)$ ,  $\binom{-}{d}_p(x) = \binom{-}{u}_n(x)$ , violations of which are discussed below.)

Kulagin [26] has recently noted that NuTeV's measurement of the neutron excess correction in  $\sin^2\theta_W$ , 0.0080, does not agree with the correction of the effect in  $R^-$ , and suggests that the difference could be taken as a (substantial) correction to the NuTeV measurement. However, the differences can be partly understood in terms of the experimental cuts discussed in Section 4.2 which reduce the neutron excess correction by 20%, and partly understood as the differences between the NuTeV 1C fit and  $R^-$ . Therefore, the suggestion by Kulagin that this difference is a correction to NuTeV's  $\sin^2\theta_W$  is incorrect.

Global analyses of unpolarized parton distributions usually assume no strange asymmetry, i.e. imposing as a constraint  $s(x) = \bar{s}(x)$ . Moreover, a fit ansatz like [27]

$$s(x) = \bar{s}(x) = \kappa \frac{\bar{u}(x) + \bar{d}(x)}{2}, \quad (4.13)$$

ties the strangeness distribution to the relatively well known  $\bar{u}(x)$  and  $\bar{d}(x)$  distributions, thereby underestimating the true uncertainty [28]. There are several recent dedicated analyses of inclusive lepton-nucleon DIS (including neutrino data) [29, 30, 31], which have used various methods to account for the uncertainties and correlated errors in parton distributions [30], [32].

One of these analyses [29] of the CDHS neutrino data and charged-lepton data reported some improvement in their fits if they allow for an asymmetry in the strange sea at high  $x$ . However, this large asymmetry at high  $x$  is directly excluded by the non-observation of high  $x$  dimuon events at NuTeV and CCFR [33]. An update of this analysis using CCFR and CDHS charged-current neutrino data no longer finds the large significant asymmetry between the strange and anti-strange quark distributions [34].

As illustrated above, the NuTeV dimuon data [33] can help in understanding the quark flavor content of the nucleon as it provides separated measurements of  $s(x)$  and  $\bar{s}(x)$  initial state contributions to charm production.

NuTeV has measured possible differences between  $s(x)$  and  $\bar{s}(x)$  from the CCFR and NuTeV data on  $\nu_N, \bar{\nu}_N \rightarrow \mu^+ \mu^- X$  within the NuTeV enhanced LO cross-section model used in the  $\sin^2 \theta_W$  analysis. Denote the momentum integrals of the strange and anti-strange seas as  $S, \bar{S}$ , i.e.,  $S = \int x s(x) dx$  and  $\bar{S} = \int x \bar{s}(x) dx$ . Within this model, the dimuon data implies a *negative* asymmetry [22],

$$S - \bar{S} = -0.0027 \pm 0.0013, \quad (4.14)$$

or an asymmetry of  $11 \pm 6\%$  of  $(S + \bar{S})$ . Therefore, dropping the assumption of strange-antistrange symmetry results in an *increase* in the NuTeV value of  $\sin^2 \theta_W$ ,

$$\Delta \sin^2 \theta_W = +0.0020 \pm 0.0009. \quad (4.15)$$

The initial NuTeV measurement, which assumes  $s(x) = \bar{s}(x)$ , becomes

$$\sin^2 \theta_W^{(\text{on-shell})} = 0.2297 \pm 0.0019. \quad (4.16)$$

A preliminary analysis of the strange and anti-strange asymmetry in an NLO cross-section model also finds the momentum carried by the seas to be consistent within uncertainties. It is worth noting that these fits have been criticized in the literature [11] because of their assumed functional form in  $x$ , and indeed, NuTeV is planning to reanalyze this data with functional forms more suggestive of strange and anti-strange asymmetries suggested by non-perturbative calculations [35, 36, 37, 38].

The impact of uncertainties in the strange-antistrange and in the up-down quark asymmetries of the target on the NuTeV measurement of  $\sin^2 \theta_W$  has been quantified in terms of an error functional [22],  $F[\sin^2 \theta_W, \delta; x]$  such that

$$\Delta \sin^2 \theta_W = \int_0^1 F[\sin^2 \theta_W, \delta; x] \delta(x) dx, \quad (4.17)$$

for any symmetry violation  $\delta(x)$  in PDFs. All of the details of the NuTeV analysis are included in the numerical evaluation of the functionals shown in Figure 6. For this analysis, it can be seen that the level of isospin violation required to shift the  $\sin^2 \theta_W$  measured by NuTeV to its standard model expectation would be, e.g.,  $\int x (d_p(x) - u_n(x)) dx \sim 0.01$  (about 5% of  $\int x (d_p(x) + u_n(x)) dx$ ), and that the level of asymmetry in the strange sea required would be  $S - \bar{S} \sim +0.007$  (about 30% of  $S + \bar{S}$ ).

#### 4.4 Charged current charm production

Thus far, the discussion of QCD corrections to  $R^-$  as in Eqns. (4.1), (4.4) has assumed quarks to be massless. However, an important contribution to the charged current reactions is the deep-inelastic charm production in  $\nu s \rightarrow \mu^- c X$ . Clearly, the mass  $m_c$  of the charm quark should to be taken into account.

For the center-of-mass energies accessible to NuTeV, a scheme of three light flavors in the nucleon is expected to give an appropriate approximation. Thus, charm quarks are entirely generated perturbatively. The leading order QCD improved parton model then requires the

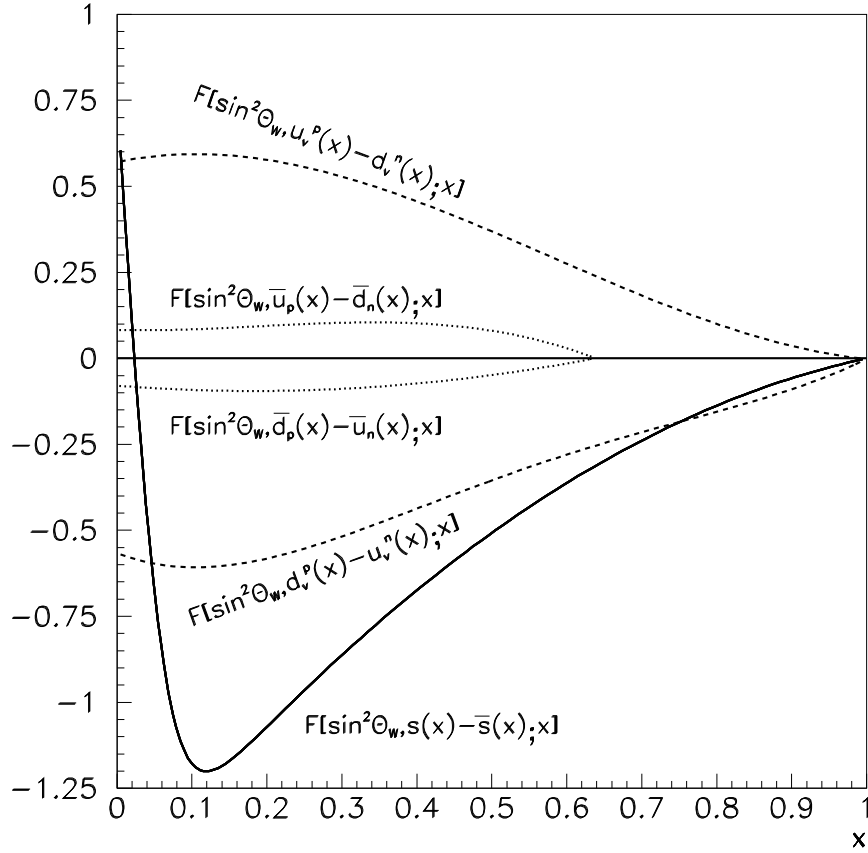


Figure 6: The functionals describing the shift in the NuTeV  $\sin^2 \theta_W$  caused by not correcting the NuTeV analysis for isospin violating  $u$  and  $d$  valence and sea distributions or for  $\langle s(x) \rangle \neq \langle \bar{s}(x) \rangle$ . The shift in  $\sin^2 \theta_W$  is determined by convolving the asymmetric momentum distribution with the plotted functional.

$x$ -dependence to change slightly. The relevant strange distribution becomes  $s(\xi, \mu_f^2)$ , where  $\xi = x(1 + m_c^2/Q^2)$  as the scaling variable correctly accounts for the single-charm threshold condition. This amounts to the so-called “slow rescaling” [39]. This, for instance, has been implemented in the NuTeV analysis of the dimuon production cross-section [33].

Also the higher order QCD corrections to  $\nu s \rightarrow \mu^- c X$  are known since long. At order  $\alpha_s$ , the complete corrections to deep-inelastic charged current scattering have been calculated [39, 40]. From these results, it is straight forward to obtain the complete  $m_c$ -dependence of  $R^-$  at NLO. However, for the purpose of this letter we restrict ourselves to a discussion of certain qualitative features. First of all, for an observable like  $R^-$ , consisting of a particular combination of total cross-sections, some dependence on charm mass cancels. Most prominently, there will be no large logarithms  $\ln(Q^2/m_c^2)$  in the NLO corrections to  $R^-$  due to the combination of coefficient functions in Eqn. (4.3). In comparison with Eqn. (4.1), the treatment of charm as a massive quark will at most introduce additional terms of order  $m_c^2/Q^2$  in the coefficients proportional to  $\alpha_s$ .

At order  $\alpha_s^2$ , only those corrections for deep-inelastic charged current scattering are known, which are logarithmically enhanced by  $\mathcal{O}(\alpha_s^2 \ln^n(Q^2/m_c^2))$  contributions [41]. For  $R^-$  this implies, that there can be at most single logarithms  $\ln(Q^2/m_c^2)$  at NNLO due to the absence of logarithmic enhanced terms at NLO.

Thus, we conclude that for  $R^-$ , any dependence on the charm mass should be weak. The same conclusion also holds, if we model the effect of experimental cuts like in  $R_{\text{model}}^-$  of Eqn. (4.7). There again, the  $m_c$ -dependence enters only through additional terms of order  $m_c^2/Q^2$ .

However, as already mentioned in Section 1.1, the charm mass dependence does play a role in choosing how the experimental  $R_{\text{exp}}^\nu$  and  $R_{\text{exp}}^{\bar{\nu}}$  are combined to extract  $\sin^2 \theta_W$ . Although the result is robust over changes in this prescription, this dependence is still worth noting and may bear further investigation. Also, the extraction of the strange sea from the CCFR/NuTeV dimuon data, which is used as input to the  $\sin^2 \theta_W$  measurement has significant NLO corrections. Again, the (quark-antiquark symmetric) strange sea doesn't enter directly into  $R^-$  but does enter into the experimental combinations used in the NuTeV fits.

For a full quantitative analysis of the various experimental cuts in phase space a detailed Monte Carlo study has to be performed. This has to account also for fragmentation, which has been entirely neglected in this discussion. In particular, the fragmentation has a non-trivial effect on the visible final state energy due to the presence of the hard neutrino from the charm decay. A Monte Carlo program, which calculates the fully differential cross-sections has been provided in [42].

## 4.5 Isospin breaking

Having concluded the investigation of perturbative QCD corrections to  $R^-$  let us now turn to investigate potential nuclear effects and isospin violation.

As argued above, knowledge of the neutron excess allows for a reasonably accurate correction for the isovector part of the cross-section; however, this correction is only valid with the assumption of isospin symmetry, i.e.,  $\overset{(-)}{u}_p(x) = \overset{(-)}{d}_n(x)$ ,  $\overset{(-)}{d}_p(x) = \overset{(-)}{u}_n(x)$ . This assumption, if significantly incorrect, could produce a sizable effect in the NuTeV extraction of  $\sin^2 \theta_W$  [43, 44, 45, 11, 22, 26].

Let us briefly discuss the main proposed non-perturbative models to generate isospin violation in the nucleon [43, 44, 45]. The earliest estimate in the literature, a bag model calculation by Sather [43], predicts large valence asymmetries of opposite sign in  $u_p - d_n$  and  $d_p - u_n$  at all  $x$ , but neglects a number of effects. Most notably, the effective mass of the remnant diquark is assumed to have a  $\delta$ -function distribution. Recently, Londgergan and Thomas, revisiting their earlier calculation [44] with the fixed diquark mass in the bag model but including a number of effects neglected by Sather, including nucleon size and mass, have argued that their calculation observes the same effect as Sather [46] and that this effect is largely independent of PDFs [47], at least when the  $x$  dependence of the NuTeV acceptance [22] is neglected. However, when this same calculation is done with a smeared distribution of diquark masses [44], the dominant isospin violating effect of the minority quark distribution,  $d_p - u_n$ , is reduced at high  $x$  and the negative asymmetry at low  $x$  is found to carry more momentum. Thus including the effect of diquark smearing, the high  $x$  and low  $x$  contributions largely cancel, leaving a negligible (0.0001) shift in the NuTeV  $\sin^2 \theta_W$  [22]. The effect is also evaluated in the meson cloud model [45], and there the asymmetries are much smaller at all  $x$ , again resulting only in a small shift in  $\sin^2 \theta_W$ .

Models aside, the NuTeV data itself cannot provide a significant independent constraint on this form of isospin violation. However, if parton distributions extracted from neutrino data (on heavy targets) are used to separate sea and valence quark distributions which affect observables at hadron colliders [48], effects of isospin breaking could be seen. Therefore, global analyses of parton distributions including the possibility of isospin violation may be able to constrain this possibility further experimentally.

#### 4.6 Nuclear effects

Any nuclear effect which can be absorbed into process-independent PDFs will not affect the NuTeV result. However, several authors have recently explored the possibility that neutrino neutral and charged current reactions may see different nuclear effects and therefore influence the NuTeV result.

Thomas and Miller [49] have offered a Vector Meson Dominance (VMD) model of low  $x$  shadowing in which such an effect might arise. The NuTeV analysis, which uses  $\nu$  and  $\bar{\nu}$  data at  $\langle Q^2 \rangle$  of 25 and 16  $\text{GeV}^2$ , respectively, is far away from the VMD regime, and the effect of this VMD model is significantly smaller than stated in this analysis. The most serious flaw in the hypothesis that this accounts for the NuTeV result, however, is that it is not internally consistent with the NuTeV data. Shadowing, a low  $x$  phenomenon, largely affects the sea quark distributions which are common between  $\nu$  and  $\bar{\nu}$  cross-sections, and therefore cancel in  $R^-$ . However, the effects in  $R^\nu$  and  $R^{\bar{\nu}}$  individually are much larger than in  $R^-$  and this model *increases* the prediction for NuTeV's  $R^\nu$  and  $R^{\bar{\nu}}$  by 0.6% and 1.2%, respectively. NuTeV's  $R^\nu$  and  $R^{\bar{\nu}}$  are both below predictions and the significant discrepancy is in the  $\nu$  mode, not the  $\bar{\nu}$  “control” sample, both in serious contradiction with the prediction of the VMD model [50].

Kulagin [26] has recently investigated possibilities for process-dependent nuclear effects disrupting NuTeV due to Fermi motion, nuclear binding corrections and shadowing, and found the effects to be small. Schmidt and collaborators [51] have suggested that there may be little or no EMC effect in the neutrino charged current but the expected EMC effect suppression at high  $x$  in the neutral current. If true, this could have the right behavior and perhaps magnitude to explain the NuTeV data because of the effect at high  $x$ . Unfortunately, this mechanism would

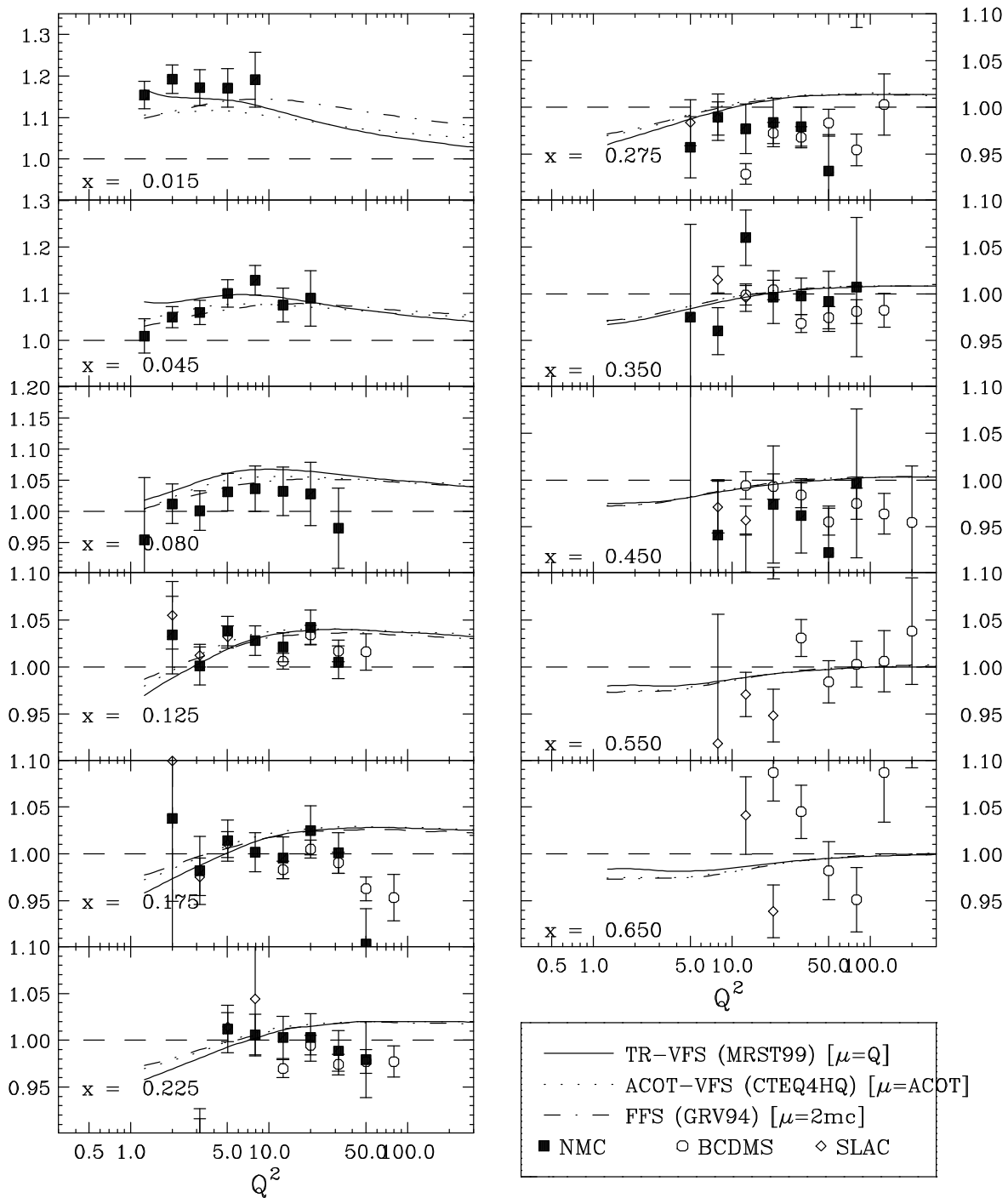


Figure 7: The ratio of  $F_2^{\nu CC}$  with a model-independent prediction from  $F_2^{\ell^\pm}$  on iron. Primarily because of quark-mass effects these ratios are not expected to be one, and different theoretical calculations for this ratio are shown. Good agreement of the ratio with expectations limits anomalous nuclear effects in the  $\nu$  charged-current interaction.

cause large differences between  $F_2^\nu$  and  $F_2^\ell$  on heavy targets at high  $x$  which are excluded by the CCFR charged current cross-section measurements [15] shown in Figure 7.

Kumano [52] has fit experimental DIS and Drell-Yan data on nuclear targets to investigate the possibility that nuclear effects are flavor dependent, rather than process dependent. Such an effect could impact NuTeV because the constraints on  $d/u$  of the nucleon come from light targets. Kumano performs these fits in the context of “nuclear PDFs”, and found very small flavor-dependent effects, except at very high  $x$  and low  $Q^2$ , a region removed by the visible energy requirement ( $E_{\text{calorimeter}} > 20 \text{ GeV}$ ) of the NuTeV analysis. The effect on the NuTeV analysis which assumes flavor-independent nuclear effects is therefore negligible.

## 5 Conclusions

Motivated by the NuTeV measurement of  $\sin^2 \theta_W$ , which deviates from the standard model prediction by approximately  $3 \sigma$ , we have studied potential sources of theoretical uncertainties. In particular, we have investigated QCD effects at higher orders in perturbation theory including the dependence on the charm mass. We have discussed the impact of parton distributions and potential nuclear effects. To assess the effect of experimental cuts on the measured  $R^-$ , we have developed a simple model  $R_{\text{model}}^-$  which accounts for  $y$ -cuts up to NLO perturbative QCD.

Based on these investigations, we conclude that higher QCD corrections are under control and small. The uncertainties on parton distributions have been discussed and will also be addressed in future global analyses. An asymmetric strange sea seems unlikely to be an explanation of the present discrepancy. Large isospin violation in parton distribution functions is a possible explanation, but the violation would have to be larger than naive estimates would suggest.

## Acknowledgements

We thank Stefano Forte and GERALYN Zeller for useful input to this work. We also thank Bogdan Dobrescu, Keith Ellis, Paolo Gambino, Sergei Kulgain, Dave Mason, Fred Olness, and Benjamin Porthault for useful discussions that have shaped the conclusions of this work. One of us (KSM) acknowledges support from the United States Department of Energy, the United States National Science Foundation and the Research Corporation of Tucson, Arizona, USA.

## Appendix

Here we give some formulae relevant for the calculation of QCD corrections to  $R^-$ . Neutral/charged current cross-sections are defined as [9]

$$\frac{d^2\sigma^{\text{NC/CC}}}{dx dy} = \frac{G_F^2}{\pi} \frac{s}{1 + Q^2/M_Z^2} k^{\text{NC/CC}}, \quad (5.1)$$

with

$$Y^+ = (1 + (1 - y)^2)/2 \quad Y^- = (1 - (1 - y)^2)/2. \quad (5.2)$$

The  $k^{\text{NC/CC}}$  in Eqn. (5.1) are expressed in terms of the structure functions  $F_2, F_3, F_L$

$$\begin{aligned}
k^{\text{NC}\nu} &= Y^+ F_2^{\text{NC}} + Y^- x F_3^{\text{NC}} - y^2/2 F_L^{\text{NC}}, \\
k^{\text{NC}\bar{\nu}} &= Y^+ F_2^{\text{NC}} - Y^- x F_3^{\text{NC}} - y^2/2 F_L^{\text{NC}}, \\
k^{\text{CC}\nu} &= Y^+ F_2^{\text{CC}} + Y^- x F_3^{\text{CC}} - y^2/2 F_L^{\text{CC}}, \\
k^{\text{CC}\bar{\nu}} &= Y^+ F_2^{\text{CC}} - Y^- x F_3^{\text{CC}} - y^2/2 F_L^{\text{CC}}.
\end{aligned} \tag{5.3}$$

For the Paschos-Wolfenstein  $R^-$ , the discussion can be restricted to the non-singlet structure functions. In the QCD improved parton model (assuming massless quarks), these are given as convolutions of parton distributions and the coefficient functions of the hard scattering process (see for instance [14, 18] or *Handbook of perturbative QCD* [53]).

$$\begin{aligned}
F_i^{\text{NC}}(x) &= x \int_x^1 \frac{dz}{z} \left\{ (u_L^2 + u_R^2)(u(z) + \bar{u}(z) + c(z) + \bar{c}(z)) \right. \\
&\quad \left. + (d_L^2 + d_R^2)(d(z) + \bar{d}(z) + s(z) + \bar{s}(z)) \right\} C_{i,q}(x/z), \\
xF_3^{\text{NC}}(x) &= x \int_x^1 \frac{dz}{z} \left\{ (u_L^2 - u_R^2)(u(z) - \bar{u}(z) + c(z) - \bar{c}(z)) \right. \\
&\quad \left. + (d_L^2 - d_R^2)(d(z) - \bar{d}(z) + s(z) - \bar{s}(z)) \right\} C_{3,q}(x/z), \\
F_i^{\text{CC}}(x) &= x \int_x^1 \frac{dz}{z} \left\{ \bar{u}(z) + d(z) + s(z) + \bar{c}(z) \right\} C_{i,q}(x/z), \\
xF_3^{\text{CC}}(x) &= x \int_x^1 \frac{dz}{z} \left\{ -\bar{u}(z) + d(z) + s(z) - \bar{c}(z) \right\} C_{3,q}(x/z), \\
F_i^{\bar{\text{CC}}}(x) &= x \int_x^1 \frac{dz}{z} \left\{ u(z) + \bar{d}(z) + \bar{s}(z) + c(z) \right\} C_{i,q}(x/z), \\
xF_3^{\bar{\text{CC}}}(x) &= x \int_x^1 \frac{dz}{z} \left\{ u(z) - \bar{d}(z) - \bar{s}(z) + c(z) \right\} C_{3,q}(x/z),
\end{aligned} \tag{5.4}$$

where  $i = 2, L$  and the non-singlet coefficient functions have an expansion in powers of  $\alpha_s$ ,

$$\begin{aligned}
C_{2,q}(x) &= \delta(1-x) + \frac{\alpha_s}{4\pi} c_{2,q}^{(1)}(x) + \frac{\alpha_s^2}{(4\pi)^2} c_{2,q}^{(2)}(x) + \dots \\
C_{3,q}(x) &= \delta(1-x) + \frac{\alpha_s}{4\pi} c_{3,q}^{(1)}(x) + \frac{\alpha_s^2}{(4\pi)^2} c_{3,q}^{(2)}(x) + \dots \\
C_{L,q}(x) &= \frac{\alpha_s}{4\pi} c_{L,q}^{(1)}(x) + \frac{\alpha_s^2}{(4\pi)^2} c_{L,q}^{(2)}(x) + \dots
\end{aligned} \tag{5.5}$$

If restricted to leading order, these equations reproduce the naive quark parton model.

In Eqns. (5.4), (5.5) all scale dependence has been suppressed. The structure functions, being observables, depend on the physical scale  $Q$ , whereas the PDFs and the coefficient functions depend on the renormalization scale  $\mu_r$  and the factorization scale  $\mu_f$ , the usual choice being  $\mu = \mu_r = \mu_f$ . Putting additionally  $\mu = Q$  also cancels all scale dependent logarithms in the coefficient functions at  $l$ -loops, i.e. all terms  $\ln^i(Q^2/\mu^2)$ ,  $i \leq l$ .

In the Paschos-Wolfenstein relation  $R^-$  only total cross-sections enter. Here, the expressions in Eqn. (5.4) simplify considerably. After the  $x$ -integration to obtain total cross-sections, all convolutions become simple products of (Mellin)-moments. Thus,

$$\int_0^1 dx F_i^{\text{NC}} = \left\{ (u_L^2 + u_R^2)(u + \bar{u} + c + \bar{c}) \right.$$

$$+(d_L^2 + d_R^2)(d + \bar{d} + s + \bar{s})\} C_{i,q}, \quad (5.6)$$

$$\int_0^1 dx x F_3^{\text{NC}}(x) = \left\{ (u_L^2 - u_R^2)(u - \bar{u} + c - \bar{c}) \right. \\ \left. + (d_L^2 - d_R^2)(d - \bar{d} + s - \bar{s}) \right\} C_{3,q}, \quad (5.7)$$

$$\int_0^1 dx F_i^{\text{CC}}(x) = \{\bar{u} + d + s + \bar{c}\} C_{i,q}, \quad (5.8)$$

$$\int_0^1 dx x F_3^{\text{CC}}(x) = \{-\bar{u} + d + s - \bar{c}\} C_{3,q}, \quad (5.9)$$

where  $i = 2, L$  and the quantities on the right hand sides are the second Mellin moments of PDFs and coefficient functions. Beyond leading order, the factorization of structure functions into PDFs and coefficient functions is arbitrary and introduces scheme dependence. The most common schemes are  $\overline{MS}$ , for which most higher order cross-sections have been calculated, and the DIS-scheme, which is physically motivated by demanding

$$C_{2,q}(x) = \delta(1-x) \quad (5.10)$$

to all orders in perturbative QCD. Of course, the PDFs and the coefficient functions change accordingly and the implications for the Paschos-Wolfenstein relation have been discussed in Section 4.

## References

- [1] E. A. Paschos and L. Wolfenstein, *Phys. Rev.* **D7**, 91 (1973).
- [2] D. Y. Bardin and V. A. Dokuchaeva, JINR-E2-86-260.
- [3] D. Y. Bardin, P. Christova, M. Jack, L. Kalinovskaya, A. Olchevski, S. Riemann and T. Riemann, *Comput. Phys. Commun.* **133**, 229 (2001).
- [4] D. Abbaneo *et al.* [The LEP Collaborations, the LEP Electroweak Working Group and the SLD Heavy Flavour and Electroweak Groups], arXiv:hep-ex/0112021.
- [5] NuTeV, G. P. Zeller *et al.*, *Phys. Rev. Lett.* **88**, 091802 (2002), hep-ex/0110059.
- [6] A. De Rujula, R. Petronzio and A. Savoy-Navarro, *Nucl. Phys. B* **154**, 394 (1979).
- [7] A. Sirlin and W. J. Marciano, *Nucl. Phys. B* **189**, 442 (1981).
- [8] S. Avvakumov *et al.*, *Phys. Rev. Lett.* **89**, 011804 (2002).
- [9] Particle Data Group, K. Hagiwara *et al.*, *Phys. Rev.* **D66**, 010001 (2002).
- [10] A. Sher *et al.*, arXiv:hep-ex/0305042.
- [11] S. Davidson, S. Forte, P. Gambino, N. Rius, and A. Strumia, *JHEP* **02**, 037 (2002), hep-ph/0112302.
- [12] S. Forte, private communication.

- [13] W. A. Bardeen, A. J. Buras, D. W. Duke, and T. Muta, *Phys. Rev.* **D18**, 3998 (1978).
- [14] W. Furmanski and R. Petronzio, *Zeit. Phys.* **C11**, 293 (1982).
- [15] CCFR/NuTeV, U.-K. Yang *et al.*, *Phys. Rev. Lett.* **86**, 2742 (2001), hep-ex/0009041.
- [16] W. L. van Neerven and E. B. Zijlstra, *Phys. Lett.* **B272**, 127 (1991).
- [17] E. B. Zijlstra and W. L. van Neerven, *Phys. Lett.* **B297**, 377 (1992).
- [18] E. B. Zijlstra and W. L. van Neerven, *Nucl. Phys.* **B383**, 525 (1992).
- [19] S. Moch and J. A. M. Vermaseren, *Nucl. Phys.* **B573**, 853 (2000), hep-ph/9912355.
- [20] W. L. van Neerven and A. Vogt, *Phys. Lett.* **B490**, 111 (2000), hep-ph/0007362.
- [21] S. Moch, J. A. M. Vermaseren, and A. Vogt, *Nucl. Phys.* **B646**, 181 (2002), hep-ph/0209100.
- [22] NuTeV, G. P. Zeller *et al.*, *Phys. Rev.* **D65**, 111103 (2002), hep-ex/0203004.
- [23] K. S. McFarland *et al.*, *Nucl. Phys. Proc. Suppl.* **112**, 226 (2002).
- [24] G. Zeller, "A precise measurement of the weak mixing angle in neutrino nucleon scattering," FERMILAB-THESIS-2002-34.
- [25] M. Arneodo *et al.* [New Muon Collaboration], *Nucl. Phys. B* **487**, 3 (1997).
- [26] S. A. Kulagin, (2003), hep-ph/0301045.
- [27] J. Pumplin *et al.*, *JHEP* **07**, 012 (2002), hep-ph/0201195.
- [28] F. Olness, Talk at DIS 2003, WG C, *XI International Workshop on Deep Inelastic Scattering* St. Petersburg, 23-27 April 2003.
- [29] V. Barone, C. Pascaud, and F. Zomer, *Eur. Phys. J.* **C12**, 243 (2000), hep-ph/9907512.
- [30] M. Botje, *Eur. Phys. J.* **C14**, 285 (2000), hep-ph/9912439.
- [31] S. I. Alekhin, *Phys. Rev.* **D63**, 094022 (2001), hep-ph/0011002.
- [32] W. T. Giele, S. A. Keller, and D. A. Kosower, (2001), hep-ph/0104052.
- [33] NuTeV, M. Goncharov *et al.*, *Phys. Rev.* **D64**, 112006 (2001), hep-ex/0102049.
- [34] B. Portheault, Talk at DIS 2003, WG A, *XI International Workshop on Deep Inelastic Scattering* St. Petersburg, 23-27 April 2003.
- [35] A. I. Signal and A. W. Thomas, *Phys. Lett. B* **191**, 205 (1987).
- [36] M. Burkardt and B. Warr, *Phys. Rev. D* **45**, 958 (1992).
- [37] S. J. Brodsky and B. Q. Ma, *Phys. Lett. B* **381**, 317 (1996).

- [38] W. Melnitchouk and M. Malheiro, Phys. Lett. B **451**, 224 (1999).
- [39] T. Gottschalk, Phys. Rev. **D23**, 56 (1981).
- [40] M. Gluck, S. Kretzer, and E. Reya, Phys. Lett. **B380**, 171 (1996), hep-ph/9603304.
- [41] M. Buza and W. L. van Neerven, Nucl. Phys. **B500**, 301 (1997), hep-ph/9702242.
- [42] S. Kretzer, D. Mason, and F. Olness, Phys. Rev. **D65**, 074010 (2002), hep-ph/0112191.
- [43] E. Sather, Phys. Lett. **B274**, 433 (1992).
- [44] E. N. Rodionov, A. W. Thomas, and J. T. Londergan, Mod. Phys. Lett. **A9**, 1799 (1994).
- [45] F.-G. Cao and A. I. Signal, Phys. Rev. **C62**, 015203 (2000), hep-ph/0001146.
- [46] J. T. Londergan and A. W. Thomas, (2003), hep-ph/0303155.
- [47] J. T. Londergan and A. W. Thomas, Phys. Lett. **B558**, 132 (2003), hep-ph/0301147.
- [48] A. Bodek, Q. Fan, M. Lancaster, K. S. McFarland, and U.-K. Yang, Phys. Rev. Lett. **83**, 2892 (1999), hep-ex/9904022.
- [49] G. A. Miller and A. W. Thomas, (2002), hep-ex/0204007.
- [50] NuTeV, G. P. Zeller *et al.*, (2002), hep-ex/0207052.
- [51] S. Kovalenko, I. Schmidt, and J.-J. Yang, Phys. Lett. **B546**, 68 (2002), hep-ph/0207158.
- [52] S. Kumano, Phys. Rev. **D66**, 111301 (2002), hep-ph/0209200.
- [53] CTEQ, R. Brock *et al.*, Rev. Mod. Phys. **67**, 157 (1995).